

Stable higher-charge vortex solitons in the cubic-quintic medium with a ring potential

LIANGWEI DONG^{1*}, MINGJING FAN², AND BORIS A. MALOMED^{3, 4}

¹Department of Physics, Zhejiang University of Science and Technology, Hangzhou, China, 310023

²Department of Physics, Shaanxi University of Science and Technology, Xi'an, China, 710021

³Department of Physical Electronics, School of Electrical Engineering, Faculty of Engineering, Tel Aviv University, Tel Aviv 69978, Israel

⁴Instituto de Alta Investigacion, Universidad de Tarapaca, Casilla 7D, Arica, Chile

*Corresponding author: dlw_0@163.com

Compiled August 23, 2023

We put forward a model for trapping stable optical vortex solitons (VSs) with high topological charges m . The cubic-quintic nonlinear medium with an imprinted ring-shaped modulation of the refractive index is shown to support two branches of VSs, which are controlled by the radius, width and depth of the modulation profile. While the lower-branch VSs are unstable in their nearly whole existence domain, the upper branch is completely stable. Vortex solitons with $m \leq 12$ obey the anti-Vakhitov-Kolokolov stability criterion. The results suggest possibilities for the creation of stable narrow optical VSs with a low power, carrying higher vorticities. © 2023 Optical Society of America

OCIS codes: (190.0190) Nonlinear optics; (190.6135) Spatial solitons; (070.7345) Wave propagation.

<http://dx.doi.org/10.1364/ao.XX.XXXXXX>

Optical vortices are a source of numerous phenomena in physics of light, displaying deep similarities to quantized vortices in superfluids and Bose-Einstein condensates (BECs) [1]. In addition to the broad phenomenology, the power profile of vortices and orbital angular momentum carried by them offer various applications, such as optical trapping, tweezers, data processing, quantum communications, etc. [2].

Self-focusing nonlinearity usually leads to azimuthal instability and splitting of vortex-carrying beams. Competing nonlinearities, which suppress the self-focusing-driven collapse, in some cases may also stabilize vortex solitons (VSs) against the spontaneous splitting [3]. Known examples include quadratic-cubic [4], cubic-quintic (CQ) [5–8] and quintic-septimal [9] optical media, with lower-order focusing and higher-order defocusing nonlinear terms. In particular, some optical materials can be accurately approximated by the CQ model [10, 11]. Competing nonlinearities also occurs in plasmas [12] and BEC [13, 14].

Relevant alternatives for trapping stable VSs are provided by confinement, with spatial modulation of the refractive index (RI) inducing an effective trapping potential [3, 15–18]. Examples include graded-index optical fibers [19], nonlinear photonic crystals with defects [20], as well as linear and nonlinear

optical lattices [21]. The trapped VSs follow the structure of the underlying RI modulation [3, 16, 17]. A similar potential profile maintains stable VSs in BEC [22].

Experimentally, robust vortex modes were observed in saturable [23] and CQ media [24, 25]. Theoretically, in most cases stable VSs were predicted with topological charge up to $m = 2$ [3, 17, 26], with a few exceptions [27–33]. In particular, in free space the 2D nonlinear Schrödinger equation (NLSE) with the CQ nonlinearity produces relatively broad stability areas for $m = 1$ and 2, and extremely narrow ones for $m \geq 3$ [7, 8], while the interplay of the harmonic-oscillator trapping potential and cubic self-focusing makes it possible to stabilize solely VSs with $m = 1$ [15]. In nonlocal media, stable higher-charge VSs can exist as a component of a vector soliton, guided by the RI profile induced by a copropagating fundamental-mode component [34, 35]. Discrete VSs with charge exceeding 2 can propagate stably in conventional [28], parity-time-symmetric [29], twisted [32], and semidiscrete [36] waveguide arrays.

The present work aims to demonstrate that stable vortex modes with higher charges can be supported by a combination of the CQ nonlinearity and an effective ring-shaped guiding potential. We find that VSs with different charges bifurcate, as lower- and upper-branch states, from the corresponding linear eigenmodes supported by the same potential. The upper-branch vortices with m up to 12 (at least) are *completely stable* in their entire existence domain. The waveguide with the required structure can be designed by means of the well-known technique used for the fabrication of multilayer optical fibers [37].

We consider the propagation of a light beam in the bulk CQ medium with the imprinted RI modulation, governed by the 2D NLSE, written in the scaled form:

$$i \frac{\partial \Psi}{\partial z} = \left[- \left(\frac{\partial^2}{\partial x^2} + \frac{\partial^2}{\partial y^2} \right) - pV(r) - |\Psi|^2 + |\Psi|^4 \right] \Psi, \quad (1)$$

Here z and (x, y) are the propagation distance and transverse coordinates, while both the cubic and quintic coefficients are scaled to be 1, without the loss of generality. As ring-shaped trapping potential is favorable for the formation of VSs, we adopt the RI modulation profile,

$$V(r) = \exp \left[- (r - r_0)^2 / d^2 \right], \quad (2)$$

where $r = \sqrt{x^2 + y^2}$, r_0 , d and p being the radius, width, and depth of the ring potential, respectively.

Stationary solutions of Eq. (1) with propagation constant b are looked for as $\Psi(x, y, z) = \psi(x, y) \exp(ibz) \equiv [\psi_r(x, y) + i\psi_i(x, y)] \exp(ibz)$, where ψ_r and ψ_i are the real and imaginary parts of the stationary mode, whose phase is $\phi = \arctan(\psi_i/\psi_r)$. The substitution of this ansatz in Eq. (1) yields a stationary equation,

$$\frac{\partial^2 \psi}{\partial x^2} + \frac{\partial^2 \psi}{\partial y^2} + pV(r)\psi - b\psi + |\psi|^2\psi - |\psi|^4\psi = 0, \quad (3)$$

which was solved by dint of the relaxation or Newton-conjugate-gradient method [38]. Parameters of the soliton families are p , r_0 , d , and b . By means of scaling, we fix $r_0 = 2\pi$ and, as a typical relevant value of the ring's width in Eq. (2), take $d = \sqrt{6}$, varying p and b to produce vortex-soliton families. Equation (1) conserves net power (norm) P , Hamiltonian H , and angular momentum M :

$$\begin{aligned} P &= \iint |\psi|^2 dx dy, \\ H &= \iint \left[\left| \frac{\partial \psi}{\partial x} \right|^2 + \left| \frac{\partial \psi}{\partial y} \right|^2 + pV|\psi|^2 - \frac{1}{2}|\psi|^4 + \frac{1}{3}|\psi|^6 \right] dx dy, \\ M &= i \iint \left[\psi^* \left(y \frac{\partial}{\partial x} - x \frac{\partial}{\partial y} \right) \psi \right] dx dy \equiv i \iint \psi^* \frac{\partial}{\partial \theta} \psi dx dy, \end{aligned} \quad (4)$$

with $*$ standing for the complex conjugate. Vortex solitons with topological charge m have the form of $\Psi(x, y, z) = |\psi(x, y)| \exp(im\theta + ibz)$, which gives rise to relation $M = mP$.

The stability of the VSs was investigated by taking perturbed solutions to Eq. (1) as $\Psi(x, y, z) = [\psi(x, y) + u(x, y) \exp(\delta z) + v^*(x, y) \exp(\delta^* z)] \exp(ibz)$, where u and v are infinitesimal perturbations and δ is the instability growth rate. Linearization of Eq. (1) around ψ yields an eigenvalue problem:

$$i \begin{bmatrix} \mathcal{M}_1 & \mathcal{M}_2 \\ -\mathcal{M}_2^* & -\mathcal{M}_1^* \end{bmatrix} \begin{bmatrix} u \\ v \end{bmatrix} = \delta \begin{bmatrix} u \\ v \end{bmatrix}, \quad (5)$$

where $\mathcal{M}_1 = \partial_x^2 + \partial_y^2 + pV - b + 2|\psi|^2 - 3|\psi|^4$ and $\mathcal{M}_2 = \psi^2(1 - 2|\psi|^2)$. Equations (5) were solved by means of the Fourier collocation method [38]. Solitons may be stable if all eigenvalues δ are imaginary.

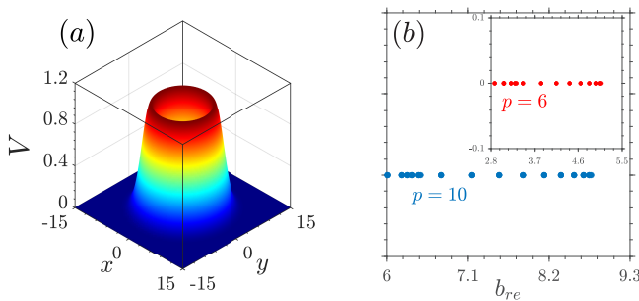


Fig. 1. (a) The ring-shaped potential (2). (b) Spectra of real eigenvalues b_{re} of the linearized equation (3) for different values of p .

First, it is relevant to produce the dispersion relation for the linear system with the ring-shaped potential (2). An example

of the potential and respective set of discrete eigenvalues, produced by the numerical solution of the linear version of Eq. (3), are shown in Figs. 1(a) and (b), where the growth of the potential's depth p results in a shift of the spectrum to the right.

In the framework of the nonlinear equation (3), fundamental and dipole solitons bifurcate, respectively, from the linear ground-state eigenmode, ψ_0 , and the degenerate pair of mutually perpendicular dipole ones representing the lowest excited states, $\psi_{1,1}$ and $\psi_{1,2}$. Vortex solitons are produced by their superposition as $\psi_{m=\pm 1} = \psi_{1,1} \pm i\psi_{1,2}$. Similarly, VSs with topological charge m bifurcate from the superposition of the m -th pair of linear eigenmodes as $\psi_{\pm m} = \psi_{m,1} \pm i\psi_{m,2}$.

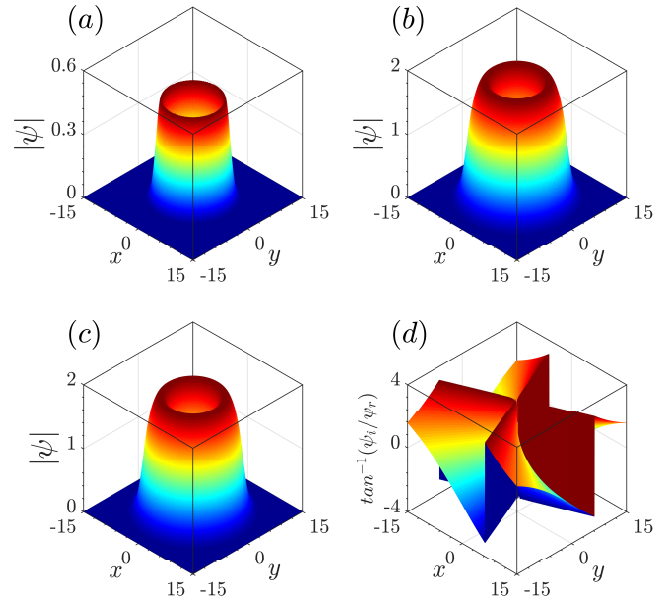


Fig. 2. Profiles of stable VSs marked in Fig. 3(a), with $m = 2$ (a,b) and $m = 4$ (c), supported by the ring potential (2) with $p = 10$ and $r_0 = 2\pi$. (d) The phase pattern corresponding to (c). The propagation constant is $b = 8.8$ (the lower branch) in (a), and 1.5 (the upper branch) in (b-d).

To build VSs, it is relevant to address the setting with the potential's depth p of the same order of magnitude as the nonlinearity strength. Representative examples of VSs with $m = 2$ and 4 are shown in Fig. 2. They exhibit a ring-shaped shape, similar to that of the potential in Fig. 1(a). Yet, the amplitude and thickness of the stable vortices vary as functions of propagation constant b , while their radius remains, naturally, close to radius r_0 of the trapping potential, unlike the strongly expanding stable VSs in the free space [7, 8].

Unlike the free-space vortices, the power P of the VSs considered here is a nonmonotonous function of b , see Fig. 3(a). For the VSs originating from the linear modes at $b = 8.674$ ($m = 2$) and $b = 8.362$ ($m = 4$), P increases with the growth of b , as long as the cubic term is the dominant one. The VS's thickness and amplitude $|\psi|_{\max}$ increase simultaneously. When $|\psi|_{\max}$ exceeds 1 (in the scaled notation adopted here), the quintic term becomes dominant, slowing the growth of $|\psi|_{\max}$ [Fig. 3(b)] and accelerating the growth of the soliton's width, $W \equiv \sqrt{\iint (x^2 + y^2) \psi^2 dx dy} / P$ [Fig. 3(c)]. The transition from the focusing to defocusing nonlinearity, along with the action of the external trapping potential, prevents the existence of VSs

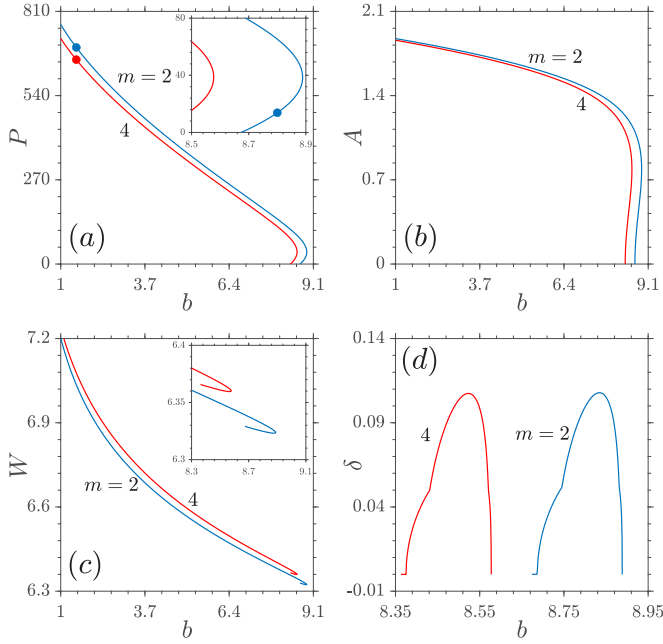


Fig. 3. (a) Power P vs. propagation constant b for VSs with $m = 2$ and 4. (b) and (c): VS amplitudes and widths for $m = 2$ and 4 vs. b . Insets in (a,c): zoom-in taken close to the cutoff (turning) point b_{cut} . (d) The instability growth rate δ vs. b for the lower VS branches. In all panels, the potential's depth is $p = 10$.

with $b > b_{\text{cut}}$ and gives rise to another branch of the VSs with the same m but the opposite sign of the slope, $dP/db < 0$. The two branches merge at the cutoff point $b = b_{\text{cut}}$ [Figs. 3(a,b)].

At fixed b , the power of the VS with $m = 2$ is slightly higher than that for $m = 4$. The difference between the amplitudes of the upper-branch VSs with $m = 2$ and 4 becomes very small as b decreases [Fig. 3(b)]. The difference between the width of the upper-branch VSs with $m = 2$ and 4 is also small, as seen in Fig. 3(c). For example, at $b = 1.5$, $|(|\psi|_{\text{max}})_{m=2} - (|\psi|_{\text{max}})_{m=4}| / (|\psi|_{\text{max}})_{m=2} = 0.0061$ and $|W_{m=2} - W_{m=4}| / W_{m=2} = 0.0077$.

The main result of this work is that the linear-stability analysis, performed on the basis of Eqs. (5), demonstrates that the ring potential helps to maintain stable VSs with $m > 2$, including large values of m . For small amplitudes $|\psi|_{\text{max}}$, one may expect that the focusing nonlinearity dominated in the lower-branch VSs, bifurcating from the linear vortex modes, makes the vortices unstable. Indeed, for VSs with $m = 2$ and 4, there is only a very narrow stability region near the linear limit, corresponding to $P \rightarrow 0$ [Fig. 3(d)]. However, for the upper-branch VSs the negative sign of dP/db provides a necessary stability condition known as the anti-Vakhitov-Kolokolov (anti-VK) stability criterion for solitons in systems dominated by self-defocusing nonlinearities [39]. Although, generally speaking, the anti-VK criterion is not sufficient for the stability, in the present case the computation of the eigenvalue spectrum produced by Eqs. (5) demonstrates that the upper branch is indeed entirely stable.

Note that the stable upper-branch vortices are narrow, and the corresponding power is not extremely high [Figs. 3(a) and (c)]. These features are in sharp contrast to the VSs in the uniform CQ medium [8], where VSs with $m > 2$ are stable only in

very narrow intervals of b , being extremely broad and carrying very high powers.

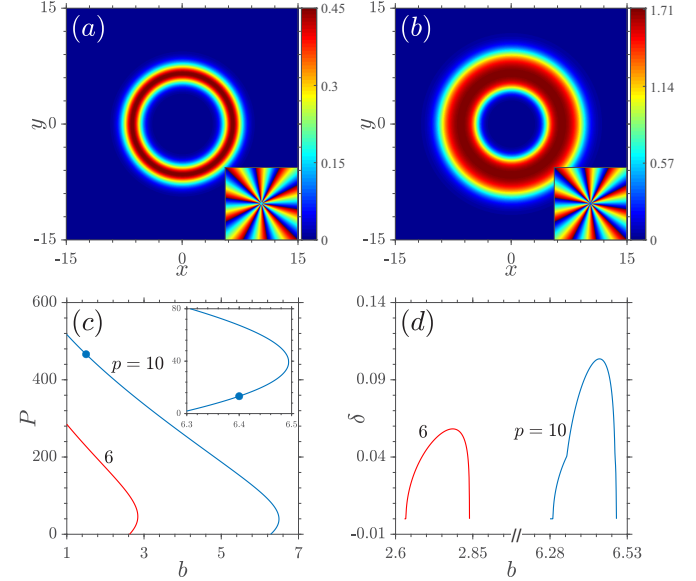


Fig. 4. (a) The map of $|\psi(x,y)|$ in an unstable VS, with $m = 10$ and $b = 6.4$, belonging to the lower branch. (b) The map for a stable VS with $m = 10$ and $b = 1.5$, belonging to the upper branch. These VSs correspond to dots in (c), i.e., to $p = 10$. Insets in (a) and (b) show the corresponding phase patterns. (c) Power P vs. b for VSs with $m = 10$, in the potential (2) with $p = 10$ and 6, respectively. Inset: zoom-in of $P(b)$ near the turning point, $b = b_{\text{cut}}$, for $p = 10$. (d) The instability growth rate δ versus b for the lower-branch VSs with $m = 10$ in the potential with $p = 10$ and 6.

Addressing the challenging issue of stable VSs with high topological charges, we have produced the solutions for up to $m = 12$, see examples for $m = 10$ in Fig. 4. Like their counterparts with lower values of m , they feature shapes of “light pipes”, confined to the narrow ring defined by the trapping potential (2), although their width and amplitude are somewhat larger, see Fig. 4(b). In accordance with what is stated above, the upper-branch VSs with $m = 10$ are stable in their entire existence domain, while their lower-branch counterparts are unstable almost everywhere.

While examples of stable VSs are presented here for $m = 2, 4, 8, 10$ and 12, the same results hold as well for odd m (at least, up to $m = 11$). On the other hand, we have checked that, if the defocusing quintic term is removed in Eq. (1), all VSs generated by the remaining cubic NLSE with the ring potential are completely unstable. Thus, the inclusion of the quintic defocusing is crucially important for the VS stability.

To verify the linear-stability predictions, we have performed systematic simulations of the perturbed evolution by means of the split-step method with the absorbing boundary conditions. To this end, the perturbed input was taken as $\Psi(x,y,z=0) = \psi(x,y)[1 + \rho(x,y)]$, where $\psi(x,y)$ is a stationary VS, and $\rho(x,y)$ is random perturbation with variance $\sigma_{\text{noise}} = 0.01$. Typical results are displayed in Fig. 5. The upper-branch stable VSs preserve their structure in the course of very long propagation, see Figs. 5(a,c,e). On the other hand, unstable lower-branch VSs break into one or more arcuate fragments [Figs. 5(b,d,f)]. The breakup distance is $z \simeq 500$ and 300 in Figs. 5(b) and (d), re-

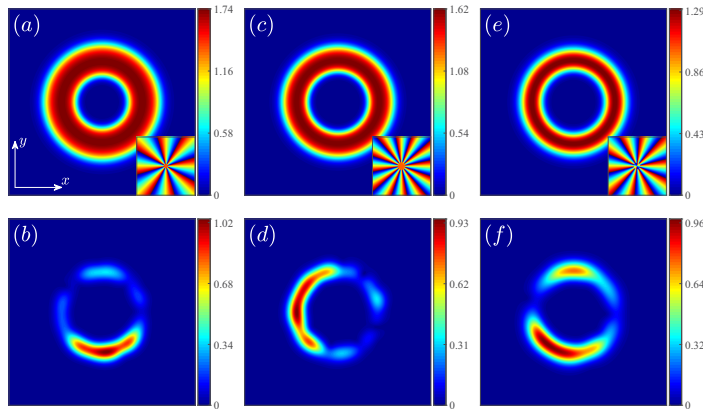


Fig. 5. The evolution of stable upper-branch (a,c,e) and unstable lower-branch (b,d,f) VSs with topological charges $m = 8$ in (a,b), 12 in (c,d), and 10 in (e,f). The propagation constant is $b = 2$ in (a,c,e), 7.3 in (b), 5.4 in (d), and 2.8 in (f). The potential depth is $p = 10$ in (a-d) and 6 in (e,f). Insets in (a,c,e) display the corresponding phase patterns. The propagation distance is $z = 2000$ and $(x, y) \in [-15, 15]$ in all panels.

spectively. Subsequently, the slightly varying fragments, which keep the angular momentum of the initial VS, circulate along the ring potential. Due to the compactness of the fragments, their amplitudes are higher than $|\psi|_{\max}$ of the input.

Finally, we discuss possibilities of the experimental creation of the predicted VSs. In particular, polydiacetylene paratoluene sulfonate (PTS) exhibits the CQ nonlinear RI, $\delta n = n_2 I - n_4 I^2$, as a function of optical intensity I [10]. At wavelength $\lambda = 1.6 \mu\text{m}$, the nonlinear indices are $n_2 = 2.2 \times 10^{-3} \text{cm}^2/\text{GW}$ and $n_4 = 0.8 \times 10^{-3} \text{cm}^4/\text{GW}^2$. The critical intensity at which δn vanishes is $I_0 = n_2/n_4 = 2.75 \text{GW}/\text{cm}^2$. Thus, the medium exhibits the self-focusing and defocusing at $I < 0.5I_0$ and $I > 0.5I_0$, respectively. The necessary ring-shaped profile of the linear refractive-index may be fabricated, as mentioned above, by means of the technology elaborated for production of composite fibers [37].

To summarize, we have found that the effective trapping potential in the form of a narrow ring, combined with the CQ nonlinearity, supports two branches of VS (vortex-solitons) families with high values of topological charge m . The radius and thickness of VSs are determined by the ring-shaped potential. While the lower-branch VSs are almost completely unstable, the upper branch is entirely stable, in sharp contrast to the VSs trapped in the harmonic-oscillator potential [33], whose stability region quickly shrinks with the growth of m . At least up to $m = 12$, the stability of all VSs fully obeys the anti-VK criterion. We thus put forward an experimentally relevant option for the creation of stable higher-charge VSs, which was not proposed previously. The results are relevant not only for optics but also for BEC, e.g., quantum droplets trapped in ring-shaped optical potentials.

Funding. Natural Science Basic Research Plan in Shaanxi Province of China (2022JZ-02); Israel Science Foundation, grant No. 1695/22.

Disclosures. The authors declare no conflicts of interest.

Data availability. Data underlying the results presented in this paper are not publicly available at this time but may be obtained from the authors upon reasonable request.

REFERENCES

1. A. S. Desyatnikov, Y. S. Kivshar, and L. Torner, *Prog. Opt.* **47**, 291–391 (2005).
2. Y. Shen, X. Wang, Z. Xie, C. Min, X. Fu, Q. Liu, M. Gong, and X. Yuan, *Light. Sci. Appl.* **8**, 90 (2019).
3. B. A. Malomed, *Phys. D: Nonlinear Phenom.* **399**, 108–137 (2019).
4. D. Mihalache, D. Mazilu, L.-C. Crasovan, I. Towers, B. A. Malomed, A. V. Buryak, L. Torner, and F. Lederer, *Phys. Rev. E* **66**, 016613 (2002).
5. M. Quiroga-Teixeiro and H. Michinel, *J. Opt. Soc. Am. B* **14**, 2004–2009 (1997).
6. V. I. Berezhiani, V. Skarka, and N. B. Aleksić, *Phys. Rev. E* **64**, 057601 (2001).
7. R. L. Pego and H. A. Warchall, *J. Nonlinear Sci.* **12**, 347–394 (2002).
8. H. Michinel, J. R. Salgueiro, and M. J. Paz-Alonso, *Phys. Rev. E* **70**, 066605 (2004).
9. A. S. Reyna, K. C. Jorge, and C. B. de Araújo, *Phys. Rev. A* **90**, 063835 (2014).
10. B. L. Lawrence and G. I. Stegeman, *Opt. Lett.* **23**, 591–593 (1998).
11. A. S. Reyna and C. B. de Araújo, *Adv. Opt. Photonics* **9**, 720–774 (2017).
12. V. E. Zakharov, V. V. Sobolev, and V. C. Synakh, *Sov. Phys. JETP* **33**, 77–81 (1971).
13. C. Josserand and S. Rica, *Phys. Rev. Lett.* **78**, 1215–1218 (1997).
14. D. S. Petrov, *Phys. Rev. Lett.* **115**, 155302 (2015).
15. D. Mihalache, D. Mazilu, B. A. Malomed, and F. Lederer, *Phys. Rev. A* **73**, 043615 (2006).
16. Y. V. Kartashov, B. A. Malomed, and L. Torner, *Rev. Mod. Phys.* **83**, 247–305 (2011).
17. B. A. Malomed, *Multidimensional Solitons* (AIP Publishing LLC, 2022).
18. F. Zhao, X. Xu, H. He, L. Zhang, Y. Zhou, Z. Chen, B. A. Malomed, and Y. Li, *Phys. Rev. Lett.* **130**, 157203 (2023).
19. S. Raghavan and G. P. Agrawal, *Opt. Commun.* **180**, 377–382 (2000).
20. A. Ferrando, M. Zacarés, P. Fernández de Córdoba, D. Binosi, and J. A. Monsoriu, *Opt. Express* **12**, 817 (2004).
21. N. Dror and B. A. Malomed, *J. Opt.* **18**, 014003 (2016).
22. K. W. Madison, F. Chevy, W. Wohlleben, and J. Dalibard, *Phys. Rev. Lett.* **84**, 806–809 (2000).
23. A. S. Reyna, G. Boudebs, B. A. Malomed, and C. B. de Araújo, *Phys. Rev. A* **93**, 013840 (2016).
24. Z. Wu, Y. Zhang, C. Yuan, F. Wen, H. Zheng, Y. Zhang, and M. Xiao, *Phys. Rev. A* **88**, 063828 (2013).
25. A. S. Reyna and C. B. de Araújo, *Opt. Lett.* **41**, 191–194 (2016).
26. J. Yang and Z. H. Musslimani, *Opt. Lett.* **28**, 2094–2096 (2003).
27. Y. V. Kartashov, A. Ferrando, A. A. Egorov, and L. Torner, *Phys. Rev. Lett.* **95**, 123902 (2005).
28. L. Dong, H. Li, C. Huang, S. Zhong, and C. Li, *Phys. Rev. A* **84**, 043830 (2011).
29. Y. V. Kartashov, V. V. Konotop, and L. Torner, *Phys. Rev. Lett.* **115**, 193902 (2015).
30. J. Qin, G. Dong, and B. A. Malomed, *Phys. Rev. A* **94**, 053611 (2016).
31. Y. Li, Z. Chen, Z. Luo, C. Huang, H. Tan, W. Pang, and B. A. Malomed, *Phys. Rev. A* **98**, 063602 (2018).
32. L. Dong, Y. V. Kartashov, L. Torner, and A. Ferrando, *Phys. Rev. Lett.* **129**, 123903 (2022).
33. D. Liu, Y. Gao, D. Fan, and L. Zhang, *Chaos Soliton. Frac.* **171**, 113422 (2023).
34. H. Zhang, Z. Weng, Q. Shou, Q. Guo, and W. Hu, *Phys. Rev. A* **101**, 033842 (2020).
35. H. Zhang, T. Zhou, and C. Dai, *Phys. Rev. A* **105**, 013520 (2022).
36. X. Zhang, X. Xu, Y. Zheng, Z. Chen, B. Liu, C. Huang, B. A. Malomed, and Y. Li, *Phys. Rev. Lett.* **123**, 133901 (2019).
37. C. Y. H. Tsao, D. N. Payne, and W. A. Gambling, *J. Opt. Soc. Am. A* **6**, 555–563 (1989).
38. J. Yang, *Nonlinear Waves in Integrable and Nonintegrable Systems* (SIAM, Philadelphia, 2010).
39. H. Sakaguchi and B. A. Malomed, *Phys. Rev. A* **81**, 013624 (2010).

References with titles

REFERENCES

1. A. S. Desyatnikov, Y. S. Kivshar, and L. Torner, "Optical vortices and vortex solitons," *Prog. Opt.* **47**, 291–391 (2005).
2. Y. Shen, X. Wang, Z. Xie, C. Min, X. Fu, Q. Liu, M. Gong, and X. Yuan, "Optical vortices 30 years on: OAM manipulation from topological charge to multiple singularities," *Light. Sci. Appl.* **8**, 90 (2019).
3. B. A. Malomed, "(invited) vortex solitons: Old results and new perspectives," *Phys. D: Nonlinear Phenom.* **399**, 108–137 (2019).
4. D. Mihalache, D. Mazilu, L.-C. Crasovan, I. Towers, B. A. Malomed, A. V. Buryak, L. Torner, and F. Lederer, "Stable three-dimensional spinning optical solitons supported by competing quadratic and cubic nonlinearities," *Phys. Rev. E* **66**, 016613 (2002).
5. M. Quiroga-Teixeiro and H. Michinel, "Stable azimuthal stationary state in quintic nonlinear optical media," *J. Opt. Soc. Am. B* **14**, 2004–2009 (1997).
6. V. I. Berezhiani, V. Skarka, and N. B. Aleksić, "Dynamics of localized and nonlocalized optical vortex solitons in cubic-quintic nonlinear media," *Phys. Rev. E* **64**, 057601 (2001).
7. R. L. Pego and H. A. Warchall, "Spectrally stable encapsulated vortices for nonlinear Schrödinger equations," *J. Nonlinear Sci.* **12**, 347–394 (2002).
8. H. Michinel, J. R. Salgueiro, and M. J. Paz-Alonso, "Square vortex solitons with a large angular momentum," *Phys. Rev. E* **70**, 066605 (2004).
9. A. S. Reyna, K. C. Jorge, and C. B. de Araújo, "Two-dimensional solitons in a quintic-septimal medium," *Phys. Rev. A* **90**, 063835 (2014).
10. B. L. Lawrence and G. I. Stegeman, "Two-dimensional bright spatial solitons stable over limited intensities and ring formation in polydiacetylene para-toluene sulfonate," *Opt. Lett.* **23**, 591–593 (1998).
11. A. S. Reyna and C. B. de Araújo, "High-order optical nonlinearities in plasmonic nanocomposites – a review", *Adv. Opt. Photonics* **9**, 720–774 (2017).
12. V. E. Zakharov, V. V. Sobolev, and V. C. Synakh, "Behavior of light beams in nonlinear media," *Sov. Phys. JETP* **33**, 77–81 (1971).
13. C. Josserand and S. Rica, "Coalescence and droplets in the subcritical nonlinear Schrödinger equation," *Phys. Rev. Lett.* **78**, 1215–1218 (1997).
14. D. S. Petrov, "Quantum mechanical stabilization of a collapsing Bose-Bose mixture," *Phys. Rev. Lett.* **115**, 155302 (2015).
15. D. Mihalache, D. Mazilu, B. A. Malomed, and F. Lederer, "Vortex stability in nearly-two-dimensional Bose-Einstein condensates with attraction", *Phys. Rev. A* **73**, 043615 (2006).
16. Y. V. Kartashov, B. A. Malomed, and L. Torner, "Solitons in nonlinear lattices," *Rev. Mod. Phys.* **83**, 247–305 (2011).
17. B. A. Malomed, *Multidimensional Solitons* (AIP Publishing LLC, 2022).
18. F. Zhao, X. Xu, H. He, L. Zhang, Y. Zhou, Z. Chen, B. A. Malomed, and Y. Li, "Vortex solitons in quasi-phase-matched photonic crystals," *Phys. Rev. Lett.* **130**, 157203 (2023).
19. S. Raghavan and G. P. Agrawal, "Spatiotemporal solitons in inhomogeneous nonlinear media," *Opt. Commun.* **180**, 377 – 382 (2000).
20. A. Ferrando, M. Zacarés, P. Fernández de Córdoba, D. Binosi, and J. A. Monsoriu, "Vortex solitons in photonic crystal fibers," *Opt. Express* **12**, 817 (2004).
21. N. Dror and B. A. Malomed, "Solitons and vortices in nonlinear potential wells," *J. Opt.* **18**, 014003 (2016).
22. K. W. Madison, F. Chevy, W. Wohlleben, and J. Dalibard, "Vortex formation in a stirred Bose-Einstein condensate," *Phys. Rev. Lett.* **84**, 806–809 (2000).
23. A. S. Reyna, G. Boudebs, B. A. Malomed, and C. B. de Araújo, "Robust self-trapping of vortex beams in a saturable optical medium," *Phys. Rev. A* **93**, 013840 (2016).
24. Z. Wu, Y. Zhang, C. Yuan, F. Wen, H. Zheng, Y. Zhang, and M. Xiao, "Cubic-quintic condensate solitons in four-wave mixing," *Phys. Rev. A* **88**, 063828 (2013).
25. A. S. Reyna and C. B. de Araújo, "Guiding and confinement of light induced by optical vortex solitons in a cubic-quintic medium," *Opt. Lett.* **41**, 191–194 (2016).
26. J. Yang and Z. H. Musslimani, "Fundamental and vortex solitons in a two-dimensional optical lattice," *Opt. Lett.* **28**, 2094–2096 (2003).
27. Y. V. Kartashov, A. Ferrando, A. A. Egorov, and L. Torner, "Soliton topology versus discrete symmetry in optical lattices," *Phys. Rev. Lett.* **95**, 123902 (2005).
28. L. Dong, H. Li, C. Huang, S. Zhong, and C. Li, "Higher-charged vortices in mixed linear-nonlinear circular arrays," *Phys. Rev. A* **84**, 043830 (2011).
29. Y. V. Kartashov, V. V. Konotop, and L. Torner, "Topological states in partially- \mathcal{PT} -symmetric azimuthal potentials," *Phys. Rev. Lett.* **115**, 193902 (2015).
30. J. Qin, G. Dong, and B. A. Malomed, "Stable giant vortex annuli in microwave-coupled atomic condensates," *Phys. Rev. A* **94**, 053611 (2016).
31. Y. Li, Z. Chen, Z. Luo, C. Huang, H. Tan, W. Pang, and B. A. Malomed, "Two-dimensional vortex quantum droplets," *Phys. Rev. A* **98**, 063602 (2018).
32. L. Dong, Y. V. Kartashov, L. Torner, and A. Ferrando, "Vortex solitons in twisted circular waveguide arrays," *Phys. Rev. Lett.* **129**, 123903 (2022).
33. D. Liu, Y. Gao, D. Fan, and L. Zhang, "Higher-charged vortex solitons in harmonic potential," *Chaos Soliton. Frac.* **171**, 113422 (2023).
34. H. Zhang, Z. Weng, Q. Shou, Q. Guo, and W. Hu, "Instability suppression of vector vortex solitons in nonlocal nonlinear media," *Phys. Rev. A* **101**, 033842 (2020).
35. H. Zhang, T. Zhou, and C. Dai, "Stabilization of higher-order vortex solitons by means of nonlocal nonlinearity," *Phys. Rev. A* **105**, 013520 (2022).
36. X. Zhang, X. Xu, Y. Zheng, Z. Chen, B. Liu, C. Huang, B. A. Malomed, and Y. Li, "Semidiscrete quantum droplets and vortices," *Phys. Rev. Lett.* **123**, 133901 (2019).
37. C. Y. H. Tsao, D. N. Payne, and W. A. Gambling, "Model characteristics of 3-layered optical fiber wave-guides – a modified approach", *J. Opt. Soc. Am. A* **6**, 555-563 (1989).
38. J. Yang, *Nonlinear Waves in Integrable and Nonintegrable Systems* (SIAM, Philadelphia, 2010).
39. H. Sakaguchi and B. A. Malomed, "Solitons in combined linear and nonlinear lattice potentials," *Phys. Rev. A* **81**, 013624 (2010).